

Latest Developments in the ARTEMISTM Core Simulator for BWR Steady-state and Transient Methodologies

Nicolas Martin¹, Michael Riedmann², Jérôme Bigot³

¹AREVA Inc. 2101 Horn Rapids Road, Richland, WA 99354, USA

²AREVA GmbH, Paul-Grossen-Str. 100, D-91052 Erlangen, Germany

³AREVA NP, 10 Rue Juliette Récamier, 69006 Lyon, France

nicolas.martin1@areva.com, michael.riedmann@areva.com, jerome.bigot@areva.com

Abstract - This paper presents recent progress made in AREVA NP's ARTEMISTM core simulator for Boiling Water Reactors (BWR) applications. It is employed together with APOLLO2-A, AREVA NP's state-of-the-art lattice physics code. The advanced two phase, three fields thermal-hydraulic F-COBRA-TFTM code has been internally coupled in ARTEMISTM specifically for handling BWR two-phase flow regimes. In addition to the introduction of an advanced spectral code and thermal-hydraulic solver, key improvements were introduced in the areas of the neutronics data model and pin power reconstruction techniques, relative to previous generation code systems. An advanced microscopic depletion model coupled with an improved spectral history representation model, developed specifically for BWR conditions, has been implemented in ARTEMISTM. This paper gives an overview of the enhancements introduced in the neutronics and thermal hydraulic computational models, along with a summary of code verification and validation accumulated against actual BWR cycles.

I. INTRODUCTION

AREVA NP has developed and extensively validated the new code system ARCADIA® for core design and safety analyses for Light Water Reactors [1]. One of the central components of this package is the ARTEMISTM [2] code, AREVA NP's LWR next generation core simulator. Lately, active development has been initiated on the BWR modeling aspect within the context of the ARCADIA® chain, where several complementary axes of development are pursued:

- Migration of the key features from the MICROBURN-B2 [3] core simulator towards ARTEMISTM, while modernizing and modularizing the software architecture of the code. ARTEMISTM is built upon the best features from several PWR core simulators, the MICROBURN-B2 BWR core simulator, and has many new models and enhancements compared to the previous generation codes. For the BWR market, the MICROBURN-B2 core simulator has been widely used for several decades in the USA, Europe, and in Asia for core design and licensing. ARTEMISTM is being developed to be its successor. By converging PWR and BWR modeling capabilities into one single code, we can leverage AREVA's worldwide validation database and extensively validate ARTEMISTM physical models.
- Extension and improvements of the physical models and solvers, to meet more demanding core operating strategies and more heterogeneous fuel design assemblies than were present several decades ago. Some of the changes introduced include extension of the cross section model to capture additional feedback parameters, improved reflector model, extension of the TIP/LPRM detector response models, extension to multigroup, availability of a semi-analytic nodal method, and improved pin power reconstruction techniques. The

thermal-hydraulic solver (3-equations model based on a homogeneous equilibrium model) from the predecessor code MICROBURN-B2 is available in ARTEMISTM for fast performance and steady-state calculations, while the newly implemented F-COBRA-TFTM solver is now available for both steady-state and transient regimes. A dedicated fuel rod model based on AREVA NP's state-of-the-art fuel performance code GALILEOTM [4] solves the conduction equation in both steady-state and transient regime.

- Unification and consolidation of 3D steady-state and 3D transient coupled neutronics and thermal-hydraulics into one single code. Most current methodologies still rely on separate codes for handling the steady-state and transient aspects. It requires an additional iterative procedure to make the initial steady-state calculation (which will serve as the start of the transient) consistent between both cases. The introduction of modern software architecture containing fully consistent steady-state and transient models remove the discontinuity existing in modeling space between core design and safety analyses. Furthermore, the availability in ARTEMISTM of hybrid OpenMP/MPI parallelism has made possible the development of fine mesh transient schemes, which remove the need for channel lumping or other sort of data collapsing that inherently introduce a loss of information.

In Section II., we will describe some of the improvements introduced in the area of the cross section model and pin power reconstruction method. Key results will be discussed on 2x2 colorset, or mini-core, calculations based on AREVA NP's ATRIUMTM11 lattices, and comparison with the reference results produced by APOLLO2-A will demonstrate the accuracy of the new model.

The BWR full core thermal-hydraulic model based on F-COBRA-TFTM is presented in Section III., along with the

newly introduced capabilities such as the quadrant sub-node concept, which allows fine radial mesh discretization. Section IV. provides key results on actual BWR cycles with comparison to detector measurements, and demonstrates the high level of accuracy for steady-state calculations.

Finally, Section VI. gives several examples of fast transient calculations using ARTEMISTM with F-COBRA-TFTM on BWR cores.

II. BWR CROSS SECTION DATA MODEL AND PIN POWER RECONSTRUCTION

1. Description of the Microscopic Depletion and Cross Section Representation Method

The BWR computational chain relies on the suite of codes APOLLO2-A/HERMES/ARTEMISTM. APOLLO2-A is the spectral code used to generate the cross sections and is based on the CEA 2.8 version [5]. The data required by the core simulator, such as the microscopic cross sections, the assembly and corner discontinuity factors, the pin form factors, the kinetic data, etc. are spatially homogenized and condensed to a few groups by APOLLO2-A. For BWR, several depletion paths are needed at different void fractions to capture historical effects on the microscopic cross sections. A recent development specific to ARTEMISTM for BWR applications relies on the addition of a dedicated controlled history feedback model, where the spectral changes induced by the presence of the control blades during depletion are taken into account for the microscopic cross sections and the pin form factors. It is based on the introduction of depletion paths where the control blade is inserted in the spectral code, together with a proper parametrization using a *controlled depletion history* parameter at the core simulator level.

It is shown to drastically improve the pin power uncertainties for sequences of control blade insertion and withdrawal, as it is discussed in the section 2. These depletion paths are then perturbed on coolant (water in the active channel) density, moderator density (water in the bypass and water channel), moderator temperature, fuel temperature, and the instantaneous presence or not of the control blade. Other parameters can be added for special purposes, such as the external water gap size to account for channel bow effects, or boron for modeling standby liquid boron injection. A multi-parameter database is then created, where the parameter mesh is for instance:

- burnup, usually from 0 to 80 GWD/T
- coolant void history, at 0, 0.4, 0.8 void fraction
- instantaneous coolant void, at 0, 0.4, 0.7, 1. void fraction
- instantaneous moderator void, at 0, 0.05, 0.1 void fraction
- fuel temperature, at 560, 900, 1500 K
- moderator temperature (e.g. 293, 365, 460 K) only needed for cold startup conditions.

- Instantaneous presence or not of the control blade, instrumentation / guide tube (TIP/LPRM), etc.
- water gap dimension changes due to channel bow.

Historical parameters, such as void history and controlled depletion history, are defined as exposure-weighted integrals of their instantaneous counterparts:

$$p^{hist} = \frac{1}{Bu} \int_0^{Bu} p^{inst} dBu \quad (1)$$

where p is either the coolant void fraction, or the fraction of control rod insertion at a given node in the core simulator.

HERMES is the interface code that processes the multi-parameter database and computes the coefficients needed for the interpolation step. The cross section representation uses a generalized B-spline approach, where the mathematical order of the representation can be arbitrarily chosen such that the user can select and easily change the mathematical order and the functional basis used for the interpolation process, as long as the APOLLO2-A calculation incorporates the required sources and/or branches. Adding and removing a parameter is also done simply via the input.

A microscopic depletion model is used in ARTEMISTM. The depletion solver allows flexibility in the choice of the nuclide chain, in such a way that the number of individual nuclides to be tracked at the nodal level of the core simulator can be arbitrarily set. An optimal choice is to track the actinides, active fission products and burnable absorbers, typically resulting in about 50 isotopes, which is tractable in a production environment thanks to the OpenMP parallelization of the Krylov subspace method used for solving the Bateman equations.

For a given reaction r (absorption, fission, scattering), and a given energy group g , the macroscopic cross section is computed using:

$$\Sigma_{r,g} = \sum_{iso=1}^{N_{iso}} N_{iso} \sigma_{r,g} + \Sigma_{res,g} \quad (2)$$

The remaining cross sections of the non-tracked isotopes are lumped into a residual isotope $\Sigma_{res,g}$.

The microscopic cross section functionalization $\sigma_{r,g}$ depends on the selected N -parameter tuple (p_1, p_2, \dots, p_N) :

$$\sigma_{r,g}(p_1, p_2, \dots, p_N) = \sum_{j=1}^{N_{cross-terms}} f_j(\sigma_{r,g,j}(p_1, p_2, \dots, p_N)) \quad (3)$$

where:

- f_j is a functional representation based on a tensor product of 1D B-splines and/or 1D polynomials.
- $\sigma_{r,g,i}$ are the fitting coefficients, computed by HERMES.
- $N_{cross-terms}$ is the total number of *cross terms* between state parameters used in the mathematical representation.

Cross terms, or combinations between parameters, are introduced optionally to reduce the dimension of the multiparameter database. If $N_{cross-terms} = 1$, then all the possible combinations between the state parameters (p_1, p_2, \dots, p_N) will be included in the cross section representation, which requires numerous APOLLO2-A calculations. The interest of using different cross terms is to capture the main dependency on the selected parameters and their combined effects on the cross sections, while excluding the irrelevant ones. For instance, some of the cross term effects between instantaneous parameters can be neglected. It allows to keep the number of APOLLO2-A calculation to a tractable level and in the same time, to preserve the required level of accuracy.

A specific treatment is usually required for the burnable absorbers such as gadolinium. ARTEMISTM relies on the so-called lumped representation for the burnable absorbers ([6]). It is also present in other core simulators ([7]). The gadolinium lumped, or effective, nuclide density is defined using:

$$N(Gd^{eff}) = 5N(Gd^{154}) + 4N(Gd^{155}) + 3N(Gd^{156}) + 2N(Gd^{157}) + N(Gd^{158}) \quad (4)$$

The effective microscopic cross section becomes:

$$\sigma_{abs,g}(Gd^{eff}) = \frac{1}{N(Gd^{eff})} \sum_{i=154}^{158} \sigma_{abs,g}(Gd^i) N(Gd^i) \quad (5)$$

The lumped isotope has the characteristics of preserving the absorption reaction rates. The time parametrization of the lumped Gd absorption cross section is not done using burnup, but rather particle density itself. It is due to the fact that the microscopic thermal cross sections of the Gd isotopes depend mostly on their particle density due to the strong spatial self-shielding.

To account for the presence of the control blades, a delta-sigma concept is used. Typically for each control blade material (CR), the controlled cross section will be constructed using:

$$\Sigma_{r,g,cont} = \Sigma_{r,g,uncont} + \Delta\Sigma_{r,g}^{CR} \quad (6)$$

The specificity of this model is that it allows to simplify the mathematical representation of the controlled cross sections compared to the uncontrolled ones. Using the notations introduced above, each term can be written separately. For the uncontrolled cross sections, usually more cross terms are selected:

$$\Sigma_{r,g,uncont} = \sum_{j=1}^{N_{cross-terms}_{uncont}} f_j(\Sigma_{r,g,j,uncont}(p_1, p_2, \dots, p_N)) \quad (7)$$

For the delta-sigma contribution, only the *differences* between the controlled and uncontrolled cross sections need to be functionalized:

$$\Delta\Sigma_{r,g}^{CR} = \sum_{j=1}^{N_{cross-terms}_{cont}} g_j(\Sigma_{r,g,j,cont}(p_1, p_2, \dots, p_N) - \Sigma_{r,g,j,uncont}(p_1, p_2, \dots, p_N)) \quad (8)$$

The advantage of such representation is that the functional representation of the delta-sigma term can be simpler than the uncontrolled one, so in practice the functional g will depend on less parameters than f . Indeed, only some cross terms are necessary to model accurately the presence of the control rods on the cross sections, and thus only a limited number of points are required at the spectral code level.

One requirement of this model is that the mathematical representation of the controlled cross sections needs to be a subset of the uncontrolled ones. It means that for each controlled calculation, an uncontrolled calculation is needed for which all the parameters are identical, which translates mathematically by requiring that $g \subset f$. Conversely, setting $g = f$ in Equations 3 and 8 means that for each uncontrolled case, a corresponding controlled case is present. Each branch is simply duplicated in the APOLLO2-A input. One additional feature in ARTEMISTM for BWR is the capability to keep track of active absorbers, such as B10 present in the B4C tubes on each wing of a cruciform control blade. It is done via the direct integration of the B10 depletion equation for each spatial region of the control blade, i.e.:

$$N_{B10}(t_{i+1}) = N_{B10}(t_i) \exp^{-\langle N_{B10}(t_i) \sigma_{B10} \Delta t_i \Phi_g \rangle} \quad (9)$$

Φ_g is the surface flux at the wing location (wide water gaps). It is then possible to account for control blade depletion effects on the delta-sigma component via the introduction of different branches at the spectral code level where the B10 content has been reduced by e.g. 15 and 30%.

The interpolation of the cross sections is done on the fly by the core simulator, using the local conditions coming from the thermal hydraulic and fuel rod solvers. The cross sections are updated prior to the flux solution, itself followed by the thermal-hydraulics / fuel rod solution.

2. Verification on a Simplified 2x2 Calculation

ARTEMISTM is verified against a colorset (or 2x2) 2D assembly APOLLO2-A calculation. Colorset calculations enable to verify the microscopic cross section model, the depletion solver, the nodal flux solver, and the dehomogenization model in ARTEMISTM against the high-order transport calculation. Thermal feedback is frozen with thermal hydraulic parameters set to nominal, core average values (such as 0.4 for the void fraction), and only burnup is varied. Reflective boundary conditions are used in both codes on the 2D geometry, without critical buckling. The lattice used for the colorset is based upon the ATRIUMTM 11 fuel assembly. There are 15 gadolinium-bearing rods (7 wt%), while the U235 enrichment varies from 3.2 to 4.95%. Figure 1 displays the resulting geometry and pin layout. This type of uranium enrichment and gadolinium poisoning is representative of a bottom lattice for an 24 months cycle design. The assemblies are placed in a scatter load configuration, meaning that the north-west and south-east regions are comprised of two fresh assemblies, while the top right and bottom left have an exposure representative of once-burnt assemblies.

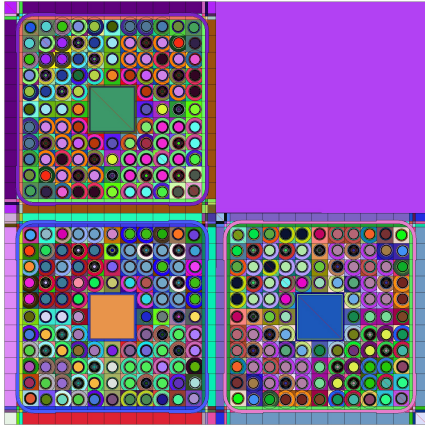


Fig. 1: ATRIUM™11 Colorset Geometry

The blade is inserted and withdrawn sequentially in the northwest corner of the top left assembly, for a duration of 5 GWD/T, which is roughly corresponding to the duration of a control rod sequence in an actual BWR in the US. It is a very important test for the pin power reconstruction method in ARTEMIS™ as the presence of the blade introduces a strong flux gradient in the node and suppresses the local thermal flux in the vicinity of the blades, which introduces an important historical effect and slows down the depletion of the burnable absorbers. Inversely, when the blade is withdrawn, pin powers close to the wide water gap will tend to spike. An accurate prediction of the local pin powers during the blade-in / blade-out sequence is of primordial importance for predicting correctly the pin LHGR, which is then used in dedicated fuel performance models to monitor pellet clad interaction.

Several models are tested in ARTEMIS™:

- Cross sections condensed to 2 energy groups without controlled depletion modeled, i.e. a dedicated depletion paths were used in APOLLO2-A and the historical parameter is present in ARTEMIS™.
- Cross sections condensed to 2 energy groups with controlled depletion modeled.
- Cross sections condensed to 4 energy groups with controlled depletion modeled.
- Cross sections condensed to 8 energy groups with controlled depletion modeled.

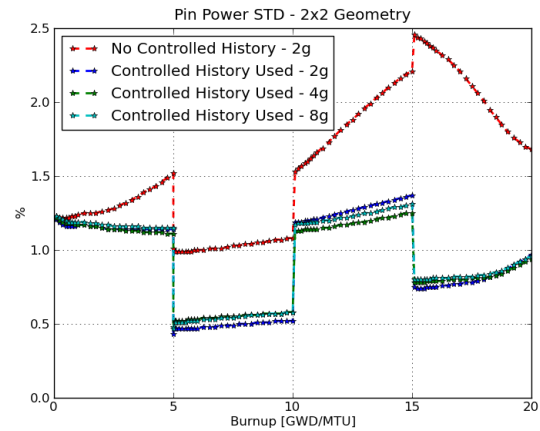


Fig. 2: Pin Power Differences between ARTEMIS™ and APOLLO2-A for the whole colorset

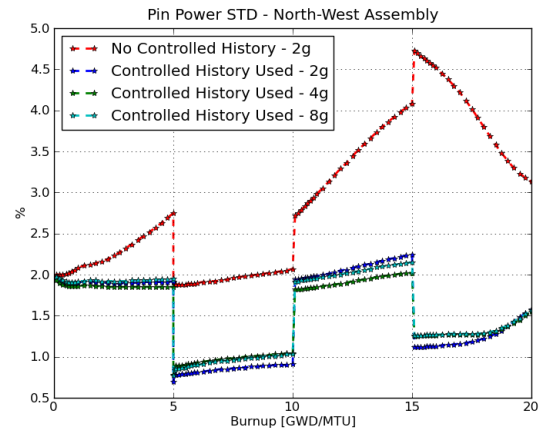


Fig. 3: Pin Power Differences between ARTEMIS™ and APOLLO2-A for the Controlled Assembly

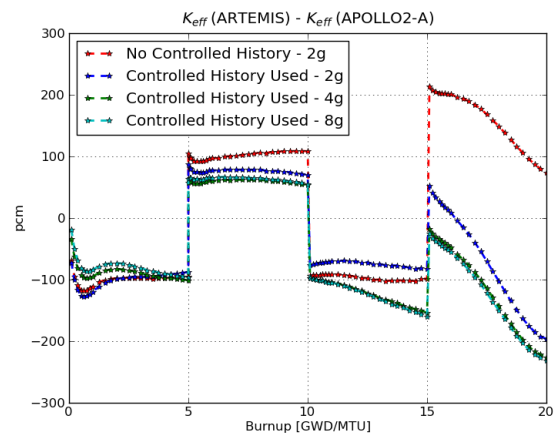


Fig. 4: Keff Differences between ARTEMIS™ and APOLLO2-A

Figure 2 displays the relative standard deviation in pin powers for the entire 2x2 geometry between ARTEMISTM and APOLLO2-A. The main difficulty in this test problem relies in modeling correctly the pin powers for the controlled assembly. Thus, Figure 3 shows the relative standard deviation only for the northwest (controlled) assembly between the pin powers calculated by ARTEMISTM and APOLLO2-A.

Overall, the eigenvalue absolute difference and the pin power standard deviations stay to within 100 pcm, and 2% with the model active, respectively. Not accounting for the controlled effect on pin powers means that the RMS error can reach up to 4.7% after the second controlled to uncontrolled sequence at 10 GWd/t. The improvement on the Keff is also demonstrated in Figure 4 albeit less significant than for the pin powers themselves. It is due to the fact that the microscopic cross section model together with the semi-analytic nodal method in ARTEMISTM can account for a significant portion of the historical effect of the controlled depletion. Finally, using 4 or even 8 energy groups slightly improves both the pin and nodal power uncertainties from ARTEMISTM, although the changes are quite small compared to the widely used 2 energy group structure. Figure 5 displays the pin power relative differences between ARTEMISTM and APOLLO2-A, at 5 GWd/t where the top left assembly goes from controlled to uncontrolled state. The controlled depletion model is used in ARTEMISTM. The same plot is made in Figure 6, without using the controlled depletion model in ARTEMISTM. The relative differences are greatly improved using the controlled depletion model. Without the controlled depletion model active, the ARTEMISTM pin powers on the left edge (facing the control blades) just after withdrawal are under-predicted by up to 5.4% (northwest corner pin), which is clearly not conservative. On the other hand, the pin power differences for the left edge stay to within 0.4 % to 1.5% using the controlled depletion model. There is also a significant improvement for the low-power, gadolinium-bearing pins where the relative differences go from 12% to less than 3.5%. Using the newly developed model reduces greatly the uncertainties, thanks to a direct representation of the controlled-to-uncontrolled feedback effect on the cross sections and pin form factors.

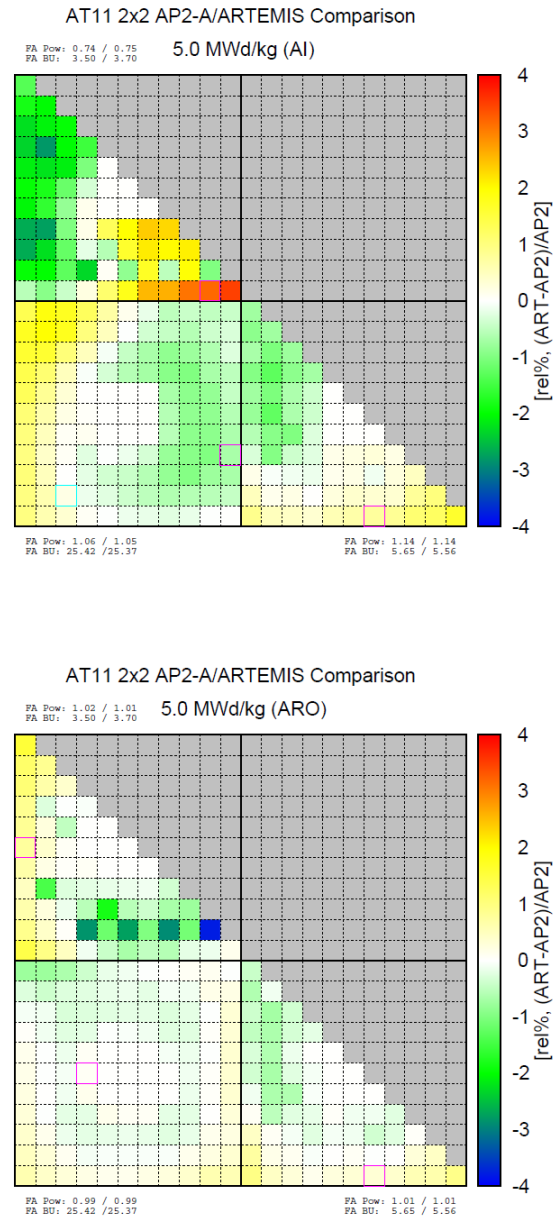


Fig. 5: Pin Power Differences at 5 GWD/T, CR inserted/withdrawn, Controlled Depletion Model On

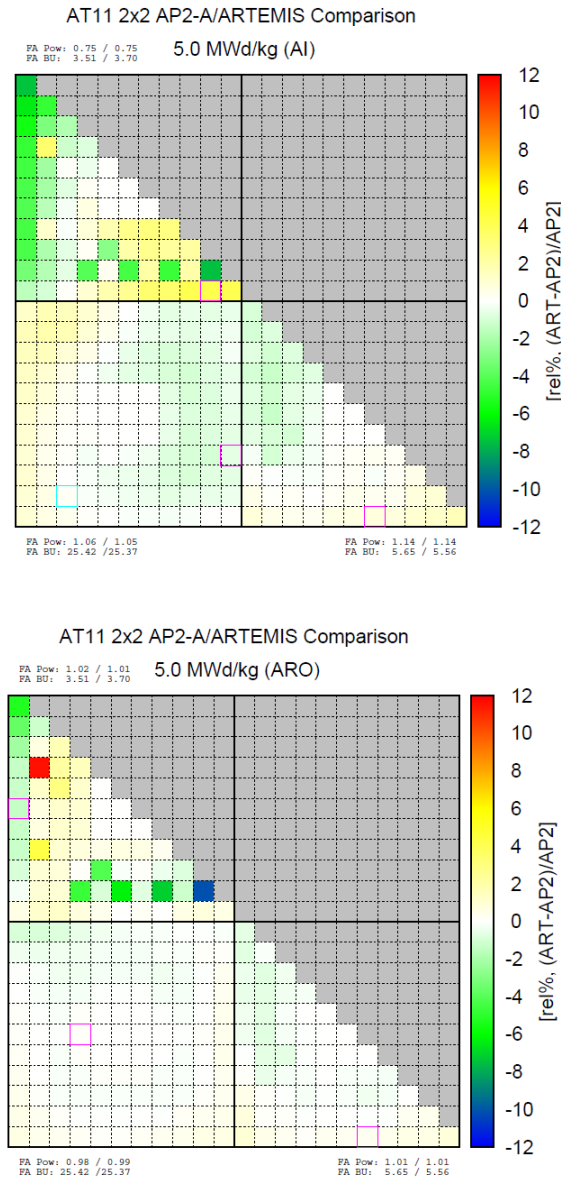


Fig. 6: Pin Power Differences at 5 GWD/T, CR inserted/withdrawn, Controlled Depletion Model Off

III. ADVANCED THERMAL HYDRAULICS MODELING

1. Presentation

F-COBRA-TFTM is based on a two fluids, three fields formulation of the two-phase flow occurring in the reactor core. Time-dependent transport equations for the mass, momentum, and energy for the continuous liquid, vapor, and entrained droplets are solved. The spatial dependency is handled through one axial and one lateral momentum equation for each field.

F-COBRA-TFTM is AREVA NP's extended version of the well-known COBRA-TF code [8], which relies on an im-

portant validation database for both PWR and BWR applications. A short list of in-house improvements to F-COBRA-TFTM is ([9], [10], [11]):

- Improvements with respect to physical models for the transition between flow regimes, turbulent mixing and void drift.
- Implementation and validation of post-dryout models.
- Validation of the void fraction, pressure drop, and critical power predicted by F-COBRA-TFTM towards AREVA NP's measurement database for the ATRIUMTM10XM and ATRIUMTM11 designs.
- Shared Memory Parallelization of the code.

In the framework of the ARTEMISTM core simulator, the input has been converted to a user friendly keyword-based format, which is converted to a XML input prior to being read by the solver.

To the authors' knowledge, this paper documents the first application of a two fluids, three fields thermal hydraulic solver to model a BWR for both steady-state and transients. Indeed, the F-COBRA-TFTM code, and its parent version, COBRA-TF, has been successfully applied for single assembly calculations both at the full channel and sub-channel level, and lately applied for full PWR core calculation through the CASL project [12] using a sub-channel discretization, but not yet to a BWR core.

Using F-COBRA-TFTM eliminates the need to rely on empirical models such as void-quality correlations, and two-phase friction multiplication factors, which are needed in legacy thermal-hydraulic solvers relying on the homogeneous equilibrium model with a drift flux approach.

The ARTEMISTM thermal hydraulic model relies on a channel per fuel assembly model, with no restrictions on the total number of assemblies in the core. The usage of such an advanced thermal-hydraulic model constitutes an important move forward from legacy thermal-hydraulic solvers relying on the homogeneous equilibrium model. On the geometrical aspect, in addition to the active channels, the internal water rod(s) present in the fuel assembly, and bypass are explicitly modeled and are treated as parallel flow paths, as depicted in Figure 7. One key difficulty for BWR is the detailed inlet region, which can includes several contributions to the bypass area (leakage paths from the channel seal, the lower tie plate holes, and from the core support plate). Different models for the bypass gaps are available, which ranges from a single, core-lumped bypass, to an individual bypass per FA, with or without cross-flow.

One key additional feature introduced here is the capability to evaluate the impact of a *quarter assembly model*. In this case the active channel is directly split into four sub-channels, with cross flow modeled optionally. It is also accompanied by a mesh refinement on the axial direction. Figure 8 gives the void fraction by quadrant for an assembly close to the periphery of the reactor core. Assemblies in the vicinity of control blades or in the core periphery are the most likely to see strong flux (or power) gradients, which inherently will induce changes in enthalpy and mass flow rates at a given radial

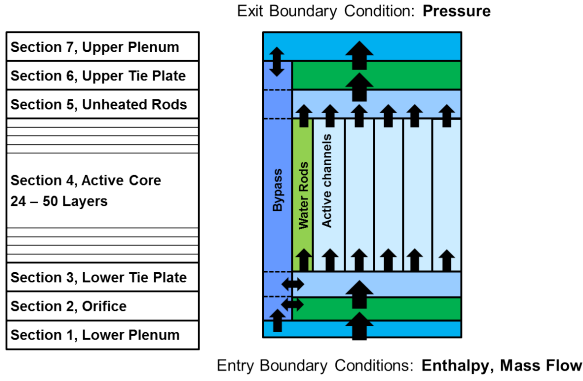


Fig. 7: BWR full core F-COBRA-TF™ Geometry

level in a fuel assembly. These variations in coolant density will themselves induce changes in the flux spectrum, that are not captured by current BWR methodologies relying solely on channel-wise thermal hydraulic calculations.

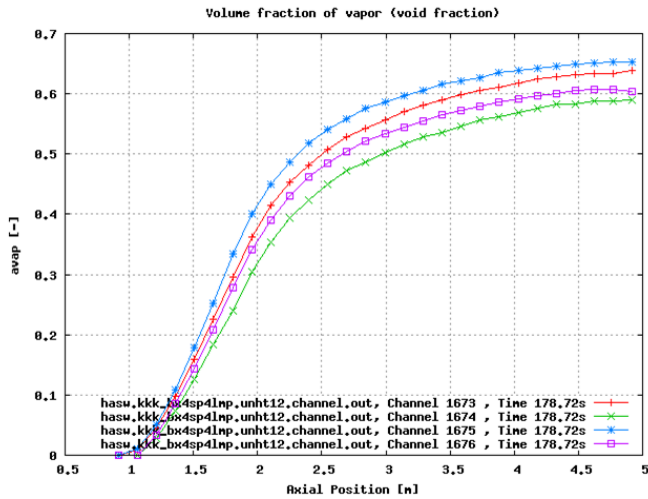


Fig. 8: Example of quadrant TH void distribution

IV. VALIDATION OF APOLLO2-A/ARTEMIS™/F-COBRA-TF™

In this section, results obtained with the new computational chain on actual BWR cycles are discussed. The reactor selected has a core size of 784 assemblies, with symmetric (C-lattice) water gaps. A combination of 9x9 and 10x10 AREVA fuel assemblies were used in these cycles. Comparison to actual in-core measurement (Traverse-in-Core Probes, TIP) is presented, along with the evolution of the hot eigenvalue versus the core operating conditions. F-COBRA-TF™ is selected as the thermal-hydraulics solver, with one channel for each fuel assembly.

In Figure 9, the eigenvalue versus burnup is displayed for cycles 9 to 16, along with the core thermal power and flow rate for each statepoint. As can be seen, the trend is fairly stable for each consecutive cycle, even when the reactor goes in coastdown at the end of the cycles. For some points, the

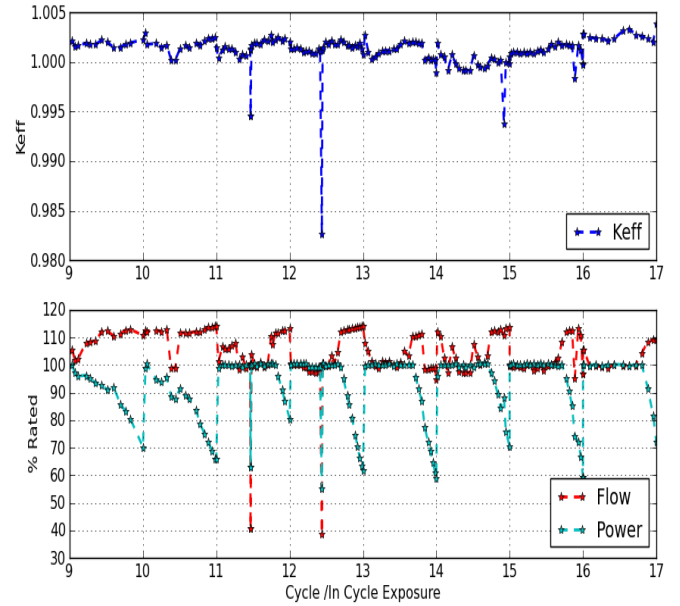


Fig. 9: Hot k_{eff} vs Burnup

Cycle	k_{eff} mean	k_{eff} STD	k_{eff} mean cycle (n) - (n - 1)
9	1.00183	0.0003	-
10	1.00066	0.0045	-0.0011
11	1.00020	0.0037	-0.0005
12	1.00023	0.0041	0.0000
13	0.99994	0.0041	-0.0003
14	0.99835	0.0048	-0.0016
15	1.00103	0.0008	0.0027
16	1.00266	0.0005	0.0016
All	1.00040	0.0037	-

TABLE I: k_{eff} Standard Deviation per Cycle

flow is fairly low (around 40% or rated), and one can see the drop in k_{eff} . Similar behavior is present in current production codes, and is expected since for these points the reactor might not be in perfect steady-state conditions. Table I shows the intra-cycle standard deviation, and the cycle-to-cycle deviation. Both values are very well behaved and the k_{eff} mean stays very close to 1 for all the cycles. Figures 10 and 11 correspond to the 2D and 3D standard deviations between the calculated and measured detector readings, respectively. Again, the points for which the reactor operates at low-flow are showing a somewhat higher deviation, which can be due to a combination of higher than expected modeling and measured uncertainties. This is certainly an area of improvements and work is pursued in this direction. Overall, the 2D and 3D TIP Standard deviations are 2.16 % and 3.78%, which are pretty good values for a BWR core simulator.

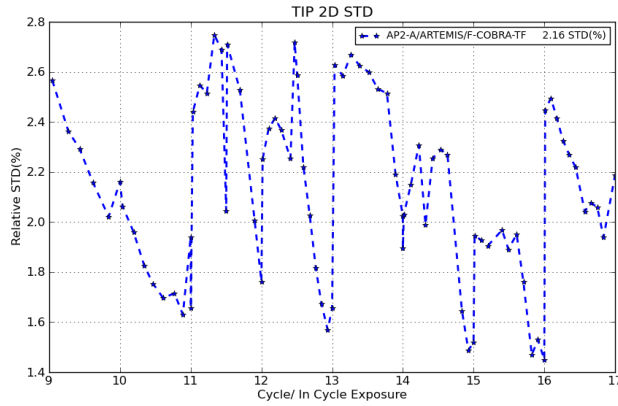


Fig. 10: TIP 2D Standard Deviation

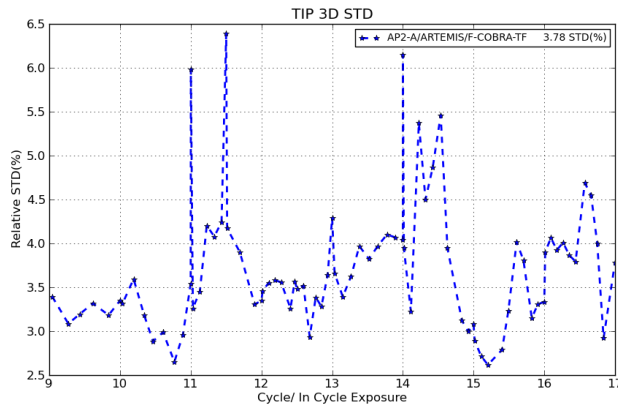


Fig. 11: TIP 3D Standard Deviation

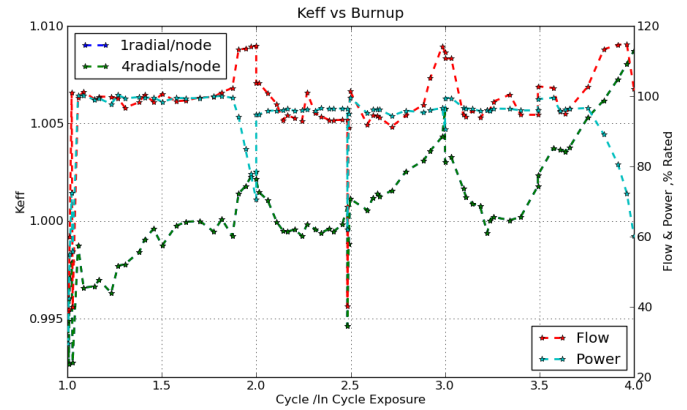


Fig. 12: Verification of the quadrant model

V. VERIFICATION OF THE QUADRANT THERMAL HYDRAULIC MODEL ON BWR CYCLE DEPLETIONS

This section documents an example of BWR cycles for which the quadrant channel TH model is enabled with F-COBRA-TFTM, and compares it to the regular channel model. Two models compared together are described here:

1. Regular model:

- one radial node per assembly.
- Spatial discretization 24 axial layers (15.46 cm spacing)
- one channel per assembly
- explicit water rod channel modeling
- one single core lumped bypass

2. Advanced Quadrant Model:

- 2x2 radial nodes per assembly.
- Spatial discretization 48 axial layers (7.73 cm spacing)
- four subchannels per assembly with cross flow enabled
- explicit water rod channel modeling
- one single core lumped bypass

If one looks at the complexity of each model in terms of number of spatial regions for thermal-hydraulics solver, the regular nodal model has about 5463 spatial regions, distributed along the 6 sections (from lower plenum to upper plenum). For the quadrant subchannel model, about 7815 spatial regions are used in F-COBRA-TFTM, with an increased number of axial layers.

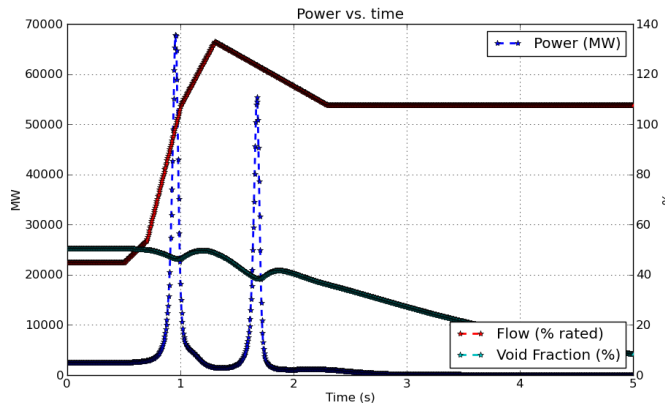


Fig. 13: Flow Runup Fast Transient

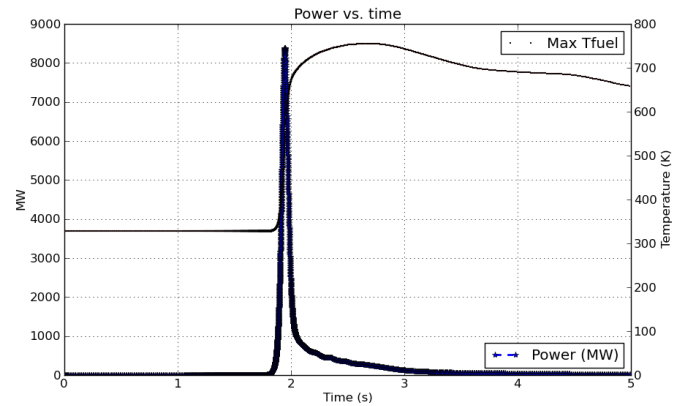


Fig. 14: Control Rod Drop Accident

VI. EXAMPLE OF TRANSIENT ANALYSES

ARTEMISTM has both steady-state and transient computational capabilities for the main physical solvers such as the neutron flux module and fuel rod module. F-COBRA-TFTM is a transient thermal-hydraulics code and thus the extension of ARTEMISTM to BWR transient regimes was a straightforward task. It is worth pointing that in this case, the steady-state solution and transient solutions are fully consistent. Indeed, previous generation code systems rely on separate codes for each application, and required some level of iterations to make the start of the transient calculation consistent with the steady-state one.

An example of a transient calculation is illustrated below in Figure 13. A fast runup of the circulation pumps, without application of the pump overspeed shutdown, is postulated. The drastic increase of mass flow rate induces a fast reactivity insertion that leads the core to be prompt-critical. The negative void feedback collapses back the void to liquid, which induces a second peak of reactivity later on. The core boundary conditions are passed to ARTEMISTM as forcing functions during the transient.

A second example of a fast transient is depicted in Figure 14. A control rod drop accident for which a fully inserted high worth control rods becomes decoupled and falls from its drive mechanism is postulated, at cold zero-power (startup) condition. The control rod is assumed to drop at its maximum speed from fully inserted to fully withdrawn. The large reactivity insertion causes the core to reach prompt criticality. The pulse in power is then terminated by the Doppler effect. No simplification is made on the geometrical modeling: a full 3D transient neutronics model is modeled, together with a full F-COBRA-TFTM model, as for regular steady-state calculations, and each fuel assembly is modeled explicitly (no channel lumping).

The two examples given in this section depict the capabilities of the ARTEMISTM core simulator with F-COBRA-TFTM to handle fast RIA transients.

VII. CONCLUSION

This paper documents key improvements made at AREVA NP in the area of BWR core physics methods, with the introduction of APOLLO2-A as the lattice physics code. F-COBRA-TFTM has been successfully applied to model whole BWR core for both stationary and transient calculations. Various improvements were made in the ARTEMISTM cross section and pin power reconstruction methodologies relative to previous BWR chains:

- Additional feedback parameters which are accounted for, e.g. bypass void feedback, explicit controlled depletion, high coolant void fraction.
- Extension from table look-up and/or low polynomials to a generalized B-spline interpolation method, which allows for additional range (e.g. up to fully voided coolant) without requiring to extrapolation.
- Extension to multigroup (e.g. > 2 energy group model).
- Fully scalable depletion solver, with extended number of isotopes tracked.
- Different representation possible for burnable absorbers, i.e. either by keeping the individual isotopes particularized or using the so-called effective isotope representation.
- Improved pin power reconstruction techniques.

Improvements to the neutronic data model are key to reduce the core simulator's uncertainties to the local (nodal or pin-wise) flux and power. These improvements are cascaded to the quantities of interest for core design and licensing, such as the thermal limits (pin or nodal Linear Heat Generation Rate, margin to CPR), and TIP/LPRM detector predictions. Note that the cross section formalism and the depletion solver are identical for both PWR and BWR, which simplifies and unifies the coding of both approaches. The main differences are purely on the parameter choice and the meshing of each parameter which are obviously different for both methodologies. Future work includes further validation on different

BWR cycles and fuel designs with F-COBRA-TFTM. Another important aspect for BWR methodologies are validation of pin power predictions against gamma scan measurements, which give an indication on the local uncertainties.

VIII. ACKNOWLEDGEMENT

We thank our colleagues from the ARTEMISTM development team for their continuous guidance, and providing the base version that served as a starting point for this project. ARCADIA, ARTEMIS, ATRIUM, F-COBRA-TF and GALILEO are trademarks or registered trademarks of AREVA NP in the U.S.A. or other countries.

REFERENCES

1. S. KUCH, M. LEBERIG, R. BROCK, F. REITERER, M. RIEDMANN, and K. ROOKS, "Transient Validation of AREVA's New ARCADIA@Code System," (July 2014), ICONE22, Prague, Czech Republic.
2. G. HOBSON, H.-W. BOLLONI, K.-A. BREITH, and D. TOMATIS, "ARTEMISTM Core Simulator: Latest Developments," (October 2013), SNA+MC 2013, Paris, France.
3. S. MISU and H. MOON, "The SIEMENS 3D Steady-State BWR Core Simulator MICROBURN-B2," (October 1998), International Conference in Nuclear Science and Technology, Long Island, NY.
4. J. STRUMPELL ET AL., "Application of GALILEO: AREVA's Advanced Fuel Performance Code and Methodology," (September 2013), LWR Fuel Performance Meeting, TopFuel 2013.
5. R. SANCHEZ ET AL., "APOLLO2 Year 2010," *Nuclear Engineering and Technology*, **42**, 5 (2010).
6. Z. WEISS, "A Consistent Definition of the Number Density of Pseudo-Isotopes," *Annals of Nuclear Energy*, pp. 153–156 (1990).
7. T. BAHADIR and S.-O. LINDAHL, "Evaluation of Rodded BWR Assembly Pin Powers with SIMULATE5," (April 2012), PHYSOR 2012, Knoxville, Tennessee, USA.
8. M. THURGOOD ET AL., "COBRA/TRAC- A Thermal-hydraulics code for Transient Analysis of Nuclear Vessels and Primary Coolant Systems,"],, NUREG/CR-3046, Pacific Northwest National Laboratory (1983).
9. M. GLÜCK, "Validation of the sub-channel code F-COBRA-TF Part I. Recalculation of single-phase and two-phase pressure loss measurements," *Nuclear Engineering and Design*, pp. 2308–2316 (2008).
10. M. GLÜCK, "Validation of the sub-channel code F-COBRA-TF Part II. Recalculation of void measurements," *Nuclear Engineering and Design*, pp. 2317–2327 (2008).
11. R. VAN GEEMERT, M. GLÜCK, M. RIEDMANN, and H. GABRIEL, "Parallelized Preconditioned BICGSTAB Solution of Sparse Linear System Equations in F-COBRA-TF," (May 2011), M&C 2011, Rio De Janeiro, Brazil.
12. R. SALKO, R. SCHMIDT, and M. AVRAMOVA, "Optimization and Parallelization of the Thermal-hydraulic Subchannel Code CTF for High-Fidelity Multi-Physics Applications," *Annals of Nuclear Energy*, pp. 122–130.